



**HAL**  
open science

## Vent temperature trends at the Vulcano Fossa fumarole field: the role of permeability

Andrew Harris, Salvatore Alparone, Alessandro Bonforte, Jonathan Dehn, Salvatore Gambino, Luigi Lodato, Letizia Spampinato

► **To cite this version:**

Andrew Harris, Salvatore Alparone, Alessandro Bonforte, Jonathan Dehn, Salvatore Gambino, et al.. Vent temperature trends at the Vulcano Fossa fumarole field: the role of permeability. *Bulletin of Volcanology*, 2012, 74, pp.1293-1311. 10.1007/s00445-012-0593-1 . hal-00787530

**HAL Id: hal-00787530**

**<https://hal.science/hal-00787530>**

Submitted on 2 Dec 2022

**HAL** is a multi-disciplinary open access archive for the deposit and dissemination of scientific research documents, whether they are published or not. The documents may come from teaching and research institutions in France or abroad, or from public or private research centers.

L'archive ouverte pluridisciplinaire **HAL**, est destinée au dépôt et à la diffusion de documents scientifiques de niveau recherche, publiés ou non, émanant des établissements d'enseignement et de recherche français ou étrangers, des laboratoires publics ou privés.



Distributed under a Creative Commons Attribution - NonCommercial 4.0 International License

# Vent temperature trends at the Vulcano Fossa fumarole field: the role of permeability

Andrew Harris · Salvatore Alparone ·  
Alessandro Bonforte · Jonathan Dehn ·  
Salvatore Gambino · Luigi Lodato · Letizia Spampinato

**Abstract** Between 1994 and 2010, we completed 16 thermal surveys of Vulcano's Fossa fumarole field (Aeolian Islands, Italy). In each survey, between 400 and 1,200 vent temperatures were collected using a thermal infrared thermometer from distances of ~1 m. The results show a general decrease in average vent temperature during 1994–2003, with the average for the entire field falling from ~220°C in 1994 to ~150°C by 2003. However, between 2004 and 2010, we witnessed heating, with the average increasing to ~190°C by 2010. Alongside these annual-scale field-wide trends, we record a spatial re-organisation of the fumarole field, characterised by shut down of vent zones towards the

crater floor, matched by rejuvenation of zones located towards the crater rim. Heating may be expected to be associated with deflation because increased amounts of vaporisation will remove volume from the hydrothermal system Gambino and Guglielmino (J Geophys Res 113: B07402, 2008). However, over the 2004–2010 heating period, no ground deformation was observed. Instead, the number of seismic events increased from a typical rate of 37 events per month during 1994–2000 to 195 events per month during 2004–2010. As part of this increase, we noticed a much greater number of high-frequency events associated with rock fracturing. We thus suggest that the heating event of 2004–2010 was the result of changed permeability conditions, rather than change in the heat supply from the deeper magmatic source. Within this scenario, cooling causes shut down of lower sectors and re-establishment of pathways located towards the crater rim, causing fracturing, increased seismicity and heat flow in these regions. This is consistent with the zone of rejuvenation (which lies towards and at the rim) being the most favourable location for fracturing given the stress field of the Fossa cone Schöpa et al. (J Volcanol Geotherm Res 203:133–145, 2011); it is also the most established zone, having been active at least since the early twentieth century. Our data show the value of deploying multi-disciplinary geophysical campaigns at degassing (fumarolic) hydrothermal systems. This allows more complete and constrained understanding of the true heat loss dynamics of the system. In the case study presented here, it allows us to distinguish true heating from apparent heating phases. While the former are triggered from the bottom-up, i.e. they are driven by increases in heat supply from the magmatic source, the latter are triggered from the top-down, i.e. by changing permeability conditions in the uppermost portion of the system to allow more efficient heat flow over zones predisposed to fracturing.

A. Harris (✉)  
Laboratoire Magmas et Volcans, Université Blaise Pascal,  
5 Rue Kessler,  
63038 Clermont Ferrand, France  
e-mail: A.Harris@opgc.univ-bpclermont.fr

S. Alparone · A. Bonforte · S. Gambino · L. Lodato ·  
L. Spampinato  
Istituto Nazionale di Geofisica  
e Vulcanologia—Sezione di Catania,  
Piazza Roma 2,  
95123 Catania, Italy

J. Dehn  
University of Alaska Fairbanks,  
903 Koyukuk Drive, P.O. Box 757320, Alaska 99775-7320, USA

L. Spampinato  
Department of Geography, University of Cambridge,  
CB2 3EN Cambridge, UK

**Keywords** Fumaroles · Vulcano · Vent temperature · Seismicity · Deformation · Permeability

## Introduction

Changes in vent temperature at active fumarole fields can be related to changes in gas geochemistry, seismic activity and ground deformation and reflect changes in input from the magmatic system, variations in system permeability and/or thermodynamics of the hydrothermal system (Falsaperla et al. 1989; Martini et al. 1991a, b; Chiodini et al. 1992a, b; Bonaccorso et al. 2010; Diliberto 2011). Of these factors, permeability can play a key role in determining the location and level of heat and gas flux at a fumarole field (Hardee 1982; Granieri et al. 2006; Aubert et al. 2008). Heating and areal growth of the fumarole field may thus result not only from increased input from the magmatic system but also from increases in system permeability (Stevenson 1993; Harris and Maciejewski 2000; Cannata et al. 2012).

Increases in system permeability may also promote increased heat, gas and fluid flow through the system, to force characteristic variations in fluid composition and ground deformation (Todesco et al. 2010). If temperatures in the system increase, then boiling and evaporation may result, with the subsequent reduction in system volume causing deflation (Gambino and Guglielmino 2008). At the same time, while characteristic high-frequency seismic signals are produced by fracturing events (which serve to increase permeability), monochromatic events can be related to crack resonance during fumarolic degassing and hence indicate enhanced, or reduced, fluid flow conditions (Alparone et al. 2010). Changes in temperature, seismicity and deformation at an active fumarole field therefore serve as important measures of the activity of the system and for understanding the system dynamics in terms of permeability and fluid flow conditions.

Between 1994 and 2010, we carried out annual vent temperature surveys at the Fossa fumarole field, located on Vulcano Island, Aeolian Islands, Italy (Fig. 1). To do this, we used thermal infrared thermometers to measure a representative sample of vents across the field (Harris and Maciejewski 2000), creating a spatial data base for vent temperature across the fumarole field spanning 16 years. Here we use these data to track the long-term temporal and spatial variations in vent temperature distribution at the field, folding in seismic and deformation time series. At Vulcano, earthquakes can be associated either with fracturing or degassing mechanisms (Cannata et al. 2012). While the first process produces volcano-tectonic events, with  $1.0 < M_d < 2.6$ , the second process can generate four classes of events, each related to dynamics occurring in the uppermost (shallow) portion of the hydrothermal system (Alparone et al. 2010). In the same

manner, patterns of ground deformation recorded at Vulcano have been interpreted as resulting either from the regional tectonic regime (Bonforte and Guglielmino 2008), this being the dominant influence, or from inflation or deflation of the shallow hydrothermal system (Gambino and Guglielmino 2008). In our investigation, we focus on those seismic and deformation trends that reflect processes operating in the shallow hydrothermal system. Relation of trends apparent in the seismic and deformation data to those apparent in the thermal data allows us to assess the control of shallow system permeability in forcing the observed geophysical trends.

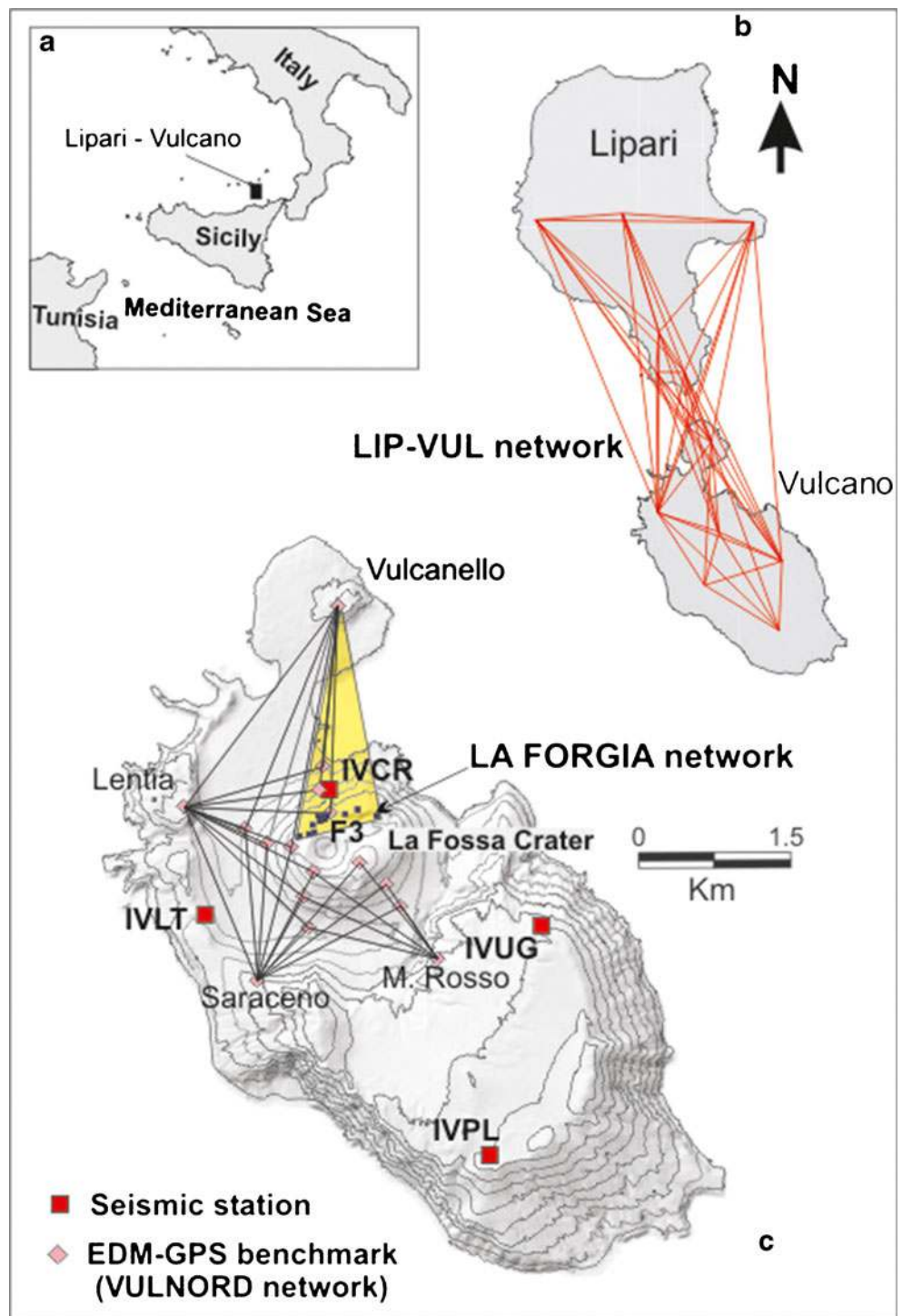
## Fumarolic activity at Vulcano and the 1994–2010 thermal surveys

Fumarolic activity has persisted at Vulcano over most of the time since the last eruption of 1888–1890. This has made Vulcano an extremely well-studied fumarolic system, as recorded by Giustolisi and de Oliveira (2005). The main fumarole field within the crater of Vulcano's Fossa cone has varied in size through time (Italiano et al. 1984; Italiano and Nuccio 1992; Bukumirovic et al. 1996, 1997). The size increased significantly, for example, between 1986 and 1995 (Fig. 2) and currently extends ~100 m along the crater rim and ~120 m from the crater rim to the crater floor (Fig. 3). Temperature variations within this field are also well documented. Sicardi (1940) reports a maximum temperature of 112°C in 1913. This, by 1924, had increased to a maximum of 615°C (Sicardi 1940). Temperatures showed further variation throughout the 1900s (Fig. 2), with a significant increase occurring during 1986–1993, when temperatures reached a maximum of ~700°C (Barberi et al. 1991; Capasso et al. 1994; Chiodini et al. 1995). This same temperature increase correlated with the increase in the field area (Fig. 2). However, five zones can be identified within the field each of which has different histories and thermal characteristics (Harris and Maciejewski 2000). These are the rim, rim rifts, upper, middle and lower zones (Fig. 3). These spatial distributions follow that expected from the stress field modelled for the Fossa cone, with fumaroles being located at concentric fractures following crater rims (especially those marking topographic highs), as well as at fractures that cut the concentric fractures obliquely (Schöpa et al. 2011). Such fractured zones mark areas of high permeability favourable for fluid ascent and fumarolic emission, thus playing a major role in controlling the main locations of high-temperature venting.

### Rim zone

The rim zone extends along the crater rim and is the oldest zone, having been active since the early 1900s (Sicardi 1940).

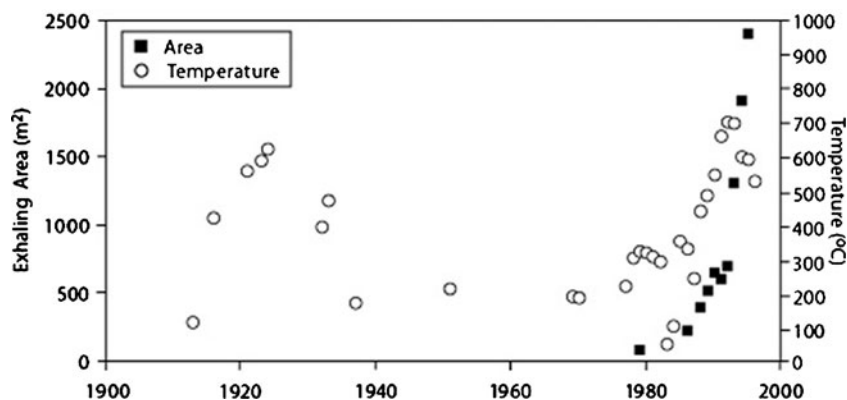
**Fig. 1** Map of the island of Vulcano, with location map for southern Italy and Lipari–Vulcano inset (a). Geodetic network covering the islands of Lipari and Vulcano (LIP–VUL network) is given in b. In c, we give the VULNORD network, plus the bench marks comprising LA FORGIA network; these are linked to the measurement monument on Vulcanello by a yellow cone. Also located are the permanent seismic stations operating on Vulcano



Maps by Italiano and Nuccio (1992) show that this zone was well established in 1984 and increased in extent between 1984 and 1987. During 1998 and 1999, this zone displayed the highest vent temperatures of the entire field, with a maximum of  $\sim 450^{\circ}\text{C}$  (Harris and Maciejewski 2000). Activity is currently concentrated along a 1–2-m-wide discontinuous, sinuous zone which extends  $\sim 200$  m along the northern sector of

the crater rim. This is one of the concentric fractures of Schöpa et al. (2011) whose location is controlled by the stress field related to the topography of the Fossa cone. As of 2005, this zone contained a mixture of low (boiling point) and higher-temperature fumaroles, with high-temperature fumaroles clustered in pits aligned along the concentric fracture to give localized hot spots aligned along the rim (Fig. 4a–c).

**Fig. 2** Plot of maximum temperature and fumarole field area as recorded in the literature between 1913 and 1996. Data base is given as supplementary material, in which the sources of each measurement are also given



### Rim rifts

The rim rifts include those fumaroles active within a zone of NW–SE trending fissures which cut the rim obliquely at the western edge of the field (Figs. 3 and 4). As such, they form one of the main oblique fracture sets of Schöpa et al. (2011) and have an en-echelon form on the outer flank. Italiano and Nuccio (1992) describe a new “very active” and roughly circular (~20 cm diameter) fumarole opening in this location in June 1987, which by November 1987 had become a “gaping fracture ~15 m long.” Oppenheimer and Rothery (1991) describe this fracture as 40 m long in 1989, and Chiodini et al. (1995) give a temperature of 310°C for a fumarole in this area during 1988. Maximum vent temperatures of ~350 to 390°C were obtained between 1994 and 1999 (Harris and Maciejewski 2000). As of 2005, relatively

high temperatures occurred along the entire length of the rift (Fig. 4d), with the main rift being ~75 m long and 0.5 m to 2.0 m wide.

### Upper zone

The upper zone is a discontinuous zone of fumaroles which currently extends ~60 m from the crater rim down into the crater across a ~170-m-wide sector (Fig. 3). Fumaroles tend to be located in isolated pits scattered across the zone, with some (but by no means all) pits being oriented along the oblique fractures of Schöpa et al. (2011). The upper zone was not indicated as active between 1984 and 1987 on maps of the field by Italiano and Nuccio (1992). Between 1994 and 1999, this zone was relatively cool, with a mean vent temperature of between 130 and 180°C and a maximum of 340°C,

**Fig. 3** Photograph of the main are of high-temperature vents of Vulcano’s Fossa cone, marking the five main zones defined in the text. Photograph is from the SW rim looking NE, line marking the rim zone covers a distance of ~200 m; distance from rim rifts to crater floor is ~150 m



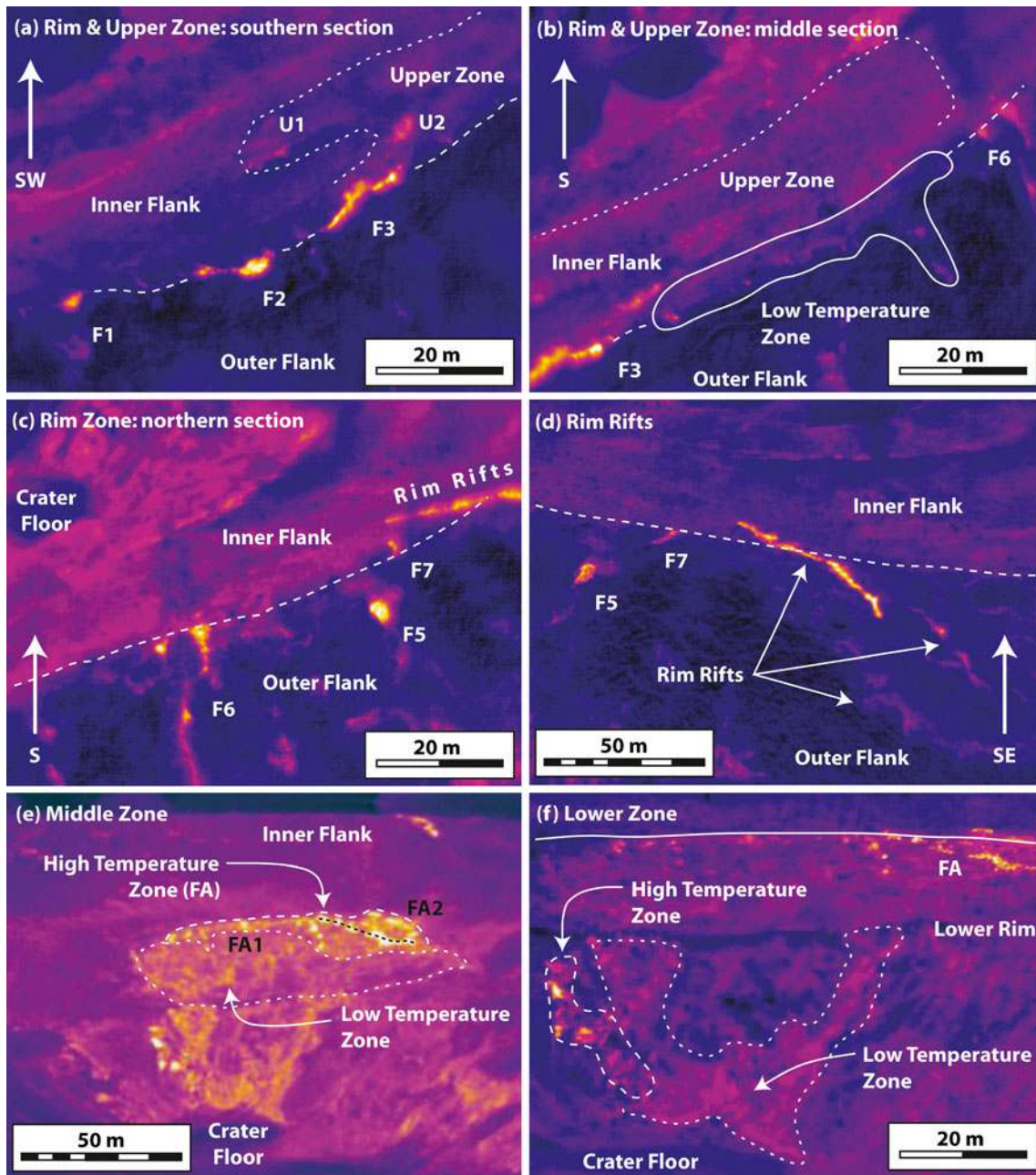


**Fig. 4** Thermal images of **a** the rim and upper zone (*southern section*), **b** the rim and upper zone (*middle section*), **c** the rim zone (*northern section*), **d** rim rifts, **e** middle zone and **f** lower zone. All images were acquired in 2005, where **a–d** are aerial oblique images acquired from a helicopter (*arrow gives view direction*). The main hot spots along the rim zone fracture are marked F1 through F7, and two hot spots

apparent in the upper zone marked U1 and U2. Crest of the rim is marked with a *dashed line*, as are the approximate limits of each fumarole main zone and sub-zone. **e**, **f** are acquired from the ground from the same vantage point as the photograph of Fig. 3. *Hotter colours* relate to higher pixel-integrated temperatures

ranking it as the coolest zone in the field during all surveys completed during that time (Harris and Maciejewski 2000).

#### Middle zone

The middle zone forms a 130×40-m zone of fumaroles on the inner flank of the crater (Fig. 3). It is another concentric

fracture zone (Schöpa et al. 2011) and appears to follow the buried line of the pre-1888 pit crater rim, whose position in this location can be inferred from sketches made by Luigi Salvatore in 1891. The extent of this zone increased markedly during the peak of thermal activity in the early 1990s. Bukumirovic et al. (1996, 1997), for example, describe expansion of a fumarole, named “FA” (see Fig. 4e for

location), within this zone from  $\sim 700 \text{ m}^2$  in 1993 to  $1,600 \text{ m}^2$  by 1994. The temperature of this zone also increased at that time. Mazor et al. (1988) gave a temperature of  $150^\circ\text{C}$  for a fumarole within this zone in 1982. Capasso et al. (1994) then described a fumarole within this zone which evolved rapidly between 1988 and 1992, with the temperature increasing from  $\sim 400$  to  $\sim 700^\circ\text{C}$ . The current upper limit of this zone is marked by a concentric fracture, cut by a SW–NE trending oblique fracture (marked FA2 on Fig. 4e). As of 2005, the high-temperature zone represented by FA was  $\sim 40 \text{ m}$  long, with the main high-temperature zone being concentrated along the 1–3-m-wide oblique fracture of FA2. Like the rim rifts, high temperatures were encountered along the entire length of the fracture. Below this is a zone of scattered low-temperature fumaroles, whose lower edge is defined by the lip of the lower (1888–1890) crater (Fig. 4e).

#### Lower zone

The lower zone is 40 to 70 m wide and extends from the lower crater rim to the crater floor. Italiano and Nuccio (1992) map no activity in this area between 1984 and 1987. Bukumirovic et al. (1997), however, map an increasing area of fumaroles in this zone from 1991. Our analyses of this sector during 2004 and 2005 (Harris et al. 2009) showed the eastern sector to be dominated by low-temperature fumaroles, with the western edge being occupied by a higher-temperature fumaroles that extended up a ravine in the lower crater wall (Fig. 4f), possibly marking the location of an oblique fracture as defined by the Schöpa et al. (2011) model. Within the high-temperature sector, maximum vent temperatures of  $390^\circ\text{C}$  were encountered in 1997 (Harris and Maciejewski 2000), declining to  $225^\circ\text{C}$  by 2004 (Harris et al. 2009).

#### Method

Our aim here is to examine, and explain, the spatial and temporal variation in vent temperature across the zones described above. To achieve this, we completed ground-based vent temperature surveys annually between 1994 and 2010, with the exceptions of 1996 and 2008–2009. In each year, between 400 and 1210 fumaroles were sampled using a hand-held thermal infrared thermometer (a Minolta/Land Cyclops 300) from a distance of  $\sim 1 \text{ m}$ . This instrument collects a spot temperature for an area defined by the instrument's one degree field of view. We corrected this brightness temperature using an emissivity of 0.97, a value obtained for surfaces within the Fossa field by Harris and Maciejewski (2000) and whose application gives a kinetic temperature that is typically within  $7^\circ\text{C}$  of thermocouple-obtained measurements for the vents (Harris and

Maciejewski 2000). The field methodology and error for these surveys is detailed in Harris and Maciejewski (2000), and summary statistics for the 1994–2010 surveys are given in Table 1. Repeat measurements on two consecutive days during the last campaign in the series (June 2010) showed that the mean and median temperature and standard deviation were more or less identical on the 2 days (Table 1), showing that our surveys were replicable. In addition, using temperature data from permanently monitored fumaroles obtained over the same measurement period, Diliberto (2011) have shown that external forces such as ambient temperature and atmospheric pressure have little influence on the measured fumarole temperature.

While the plot of mean and maximum vent temperature for the entire field during each survey is given in Fig. 5, mean and maximum vent temperatures broken out by zone are given in Fig. 6. The statistics for each zone are given in Tables 2 and 3. Following the method of Harris et al. (2009), we also produced vent temperature frequency distributions for the entire field (Fig. 7) as well as each zone (Fig. 8). High- and low-temperature fumarole zones have distinct frequency distribution characteristics that retain their shape and general form despite changes in viewing conditions and spatial resolution effects. These definitive thermal characteristics are summarized in Table 4. The shape of the histograms allows us to check any cooling or heating changes indicated by the mean and maximum temperature plots.

#### Seismic and deformation data

Trends in thermal survey time series were compared with seismic and deformation data from networks operated by the Istituto Nazionale di Geofisica e Vulcanologia—Sezione di Catania (INGV-CT). Seismic activity at Vulcano has been monitored since the 1970s by a permanent seismometer network run by the INGV-CT. The network has had several configurations, which have been developed depending on activity, and comprises four stations, as located in Fig. 1. Between 1993 and 1995, the array was upgraded, with the seismometers being replaced by three-component stations (short period Geotech S13 geophones). Between 2005 and 2007, the analogue stations were upgraded to digital stations, and the seismometers were replaced with three-component broadband Nanometrics Trillium sensors, which have flat responses in the 40- to 0.01-s period range.

Ground deformation monitoring on Vulcano began in 1975 (Bonforte and Guglielmino 2008). This involved electronic distance measurement (EDM) over a wide network covering the islands of Lipari and Vulcano (the LIP-VUL network of Fig. 1). In 1987, a local EDM network (also given in Fig. 1) was set up covering the Fossa cone, this being the VULNORD network of Fig. 1. The VULNORD network was periodically reoccupied at 4-month intervals

**Table 1** Vent temperature statistics for Vulcano Fossa fumarole field surveys, 1994 to 2010

Year	1994	1995	1997	1998	1999	2000	2001	2002a	2002b	2003	2004	2005	2006	2007	2010a	2010b
Date	October 1994	September 1995	May 1997	October 1998	June 1999	May 2000	May 2001	May 2002	September 2002	June 2003	June 2004	July 2005	June 2006	October 2007	June 2010	June 2010
No. of samples	504	485	748	1213	782	759	642	854	519	581	504	678	591	586	465	409
Min $T$ (°C)	91	59	59	60	79	55	61	73	69	74	73	72	84	72	82	82
Max $T$ (°C)	516	541	444	446	428	394	395	434	386	389	386	422	432	427	359	365
Mean $T$ (°C)	216	202	208	169	180	145	143	149	139	149	155	161	183	177	187	187
Median $T$ (°C)	198	197	195	153	171	130	131	136	109	135	134	158	186	187	198	199
Standard deviation	89	88	73	72	64	62	62	63	65	65	70	62	64	61	59	61
Standard error	4.0	4.0	2.7	2.1	2.3	2.3	2.5	2.2	2.8	2.7	3.1	2.4	2.6	2.5	2.7	3.0
Kurtosis	0.9	0.6	0.2	0.1	0.6	1.5	0.5	1.1	1.7	0.7	-0.2	0.4	0.5	-0.1	-0.5	-0.7
Skewness	1.1	0.7	0.7	0.9	0.9	1.3	0.9	1.1	1.4	1.1	0.9	0.7	0.5	0.2	-0.1	-0.2

Surveys marked 2010a and 2010b were made on consecutive days (12th and 13th June 2010, respectively) to test the repeatability of our surveys

until 1997. In May 1990, a denser array of 12 benchmarks (LA FORGIA network of Fig. 1) was installed along the northern rim of the Fossa. Distances to each benchmark were measured using EDM from a station on Vulcanello (Bonaccorso et al. 2010). For these measurements, instrumental error is 5 mm+1 ppm of the distance surveyed. This, for the VULNORD network, gives errors smaller than 0.7 cm. Since 1998, the networks have been occupied annually using GPS. Beginning in 2002, the GPS surveying strategy was improved, when 24-h-long static sessions, with 30 s acquisition rates, were completed at all stations of the LIP-VUL network and 30-min-long fast-static sessions, with 5 s acquisition rates, were carried out at all stations of the VULNORD network (Bonforte and Guglielmino 2008).

### Vent temperature trends at Vulcano: 1994–2010

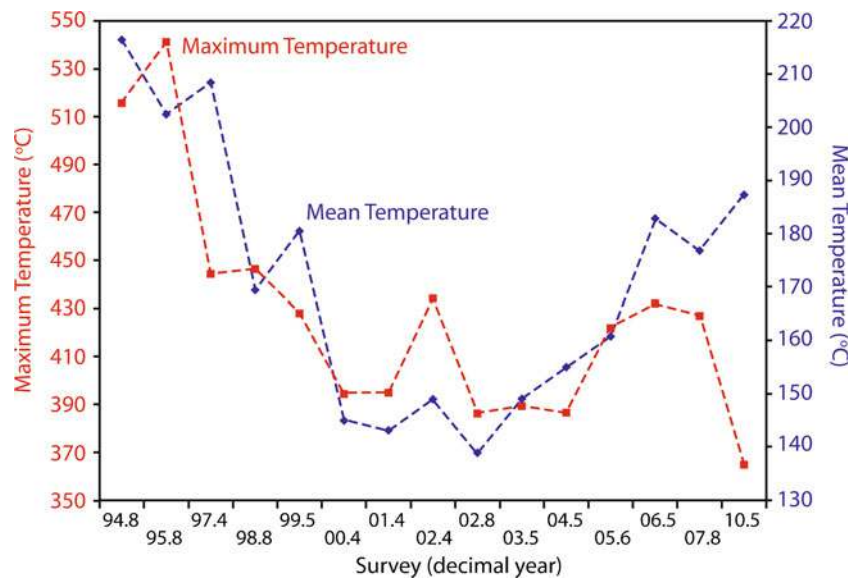
#### Field-wide trends

Plotting the maximum and mean temperature obtained during each thermal survey reveals three phases (Fig. 5): (1) a general decline in temperature during 1994 to 2000, (2) a trough between 2000 and 2003 and (3) a period of increase from 2003 to the end of the studied period in 2010. Between 1994 and 2000, a steady decline in the field-wide maximum temperature from ~550 to ~390°C was matched by a reduction in the mean from ~220 to ~140°C. A brief reversal in this declining trend is apparent in the mean data during 1999 (Fig. 5). Following 2000, both the maximum and mean temperatures remained relatively low (respectively below 430 and 160°C). An isolated peak in both the maximum and mean temperatures is evident in May 2002 (Fig. 5). An increasing trend is then evident in both the mean and maximum temperatures from 2003. This increase was expressed first in the plot of mean temperature, but was not evident until 2 years later (in 2005) in the maximum temperature plot (Fig. 5). Our final measurement of 2010 shows a decoupling between then mean and maximum temperature plots, with the mean temperature increasing by ~10°C between 2007 and 2010 and the maximum decreasing by 60°C. However, such decoupling has occurred before: the mean increasing by ~10°C between 1995 and 1997 but the maximum decreasing by ~100°C (Fig. 5).

#### Zonal trends I: the rim rifts

Examining the trends by zone reveals that the rim rifts are a relatively high-temperature group of fumaroles characterized by relatively stable temperatures, with both the maximum and mean temperature varying by less than 65°C over the 16-year measurement period (Fig. 6). The mean temperature, however, does show a steady decline from 260 to

**Fig. 5** Plot of maximum and mean temperature obtained for the entire fumarole field for each survey between 1994 and 2010 (see Table 1 for complete data set)



200°C between 1994 and 2002. Between 2002 and 2006, mean temperature remained relatively low but stable, being ~200°C in 2002 and 202°C in 2006. Thereafter, mean temperature began to climb, reaching 234°C by 2010 (Fig. 6).

#### Zonal trends II: all other zones

All other zones show a general decline in both maximum and mean temperature between 1994 and 2001 (Fig. 6). The decline in maximum temperature was similar for all zones (Table 5). In terms of mean temperature, all zones showed a decline, but this was the greatest at the middle and upper zones (Table 5). In terms of mean temperature, the upper zone appeared dead by 2001 having a mean of just 85°C, compared with 178°C in 1994, and being 36°C cooler than the next coolest zone, the lower zone (Fig. 6). However, the maximum remained at ~180°C, not reaching its trough (108°C) until 2 years later in 2003.

The turnaround to increasing temperature began first at the rim zone after 2003, with the mean increasing from 114°C in May 2003 to 203°C by May 2006. Between the same dates, the maximum increased from 315 to 432°C, transforming this zone from the third hottest to the hottest zone in the field (Fig. 6). The upper zone responded the following year, the turnaround occurring after 2004, with the mean increasing from 98°C in May 2003 to 190°C in both 2007 and 2010. At the same time, the maximum temperature increased from 108°C in 2003 to 325°C by 2007, overtaking the middle zone (containing FA) in terms of both mean and maximum temperature by 2010 (Fig. 6).

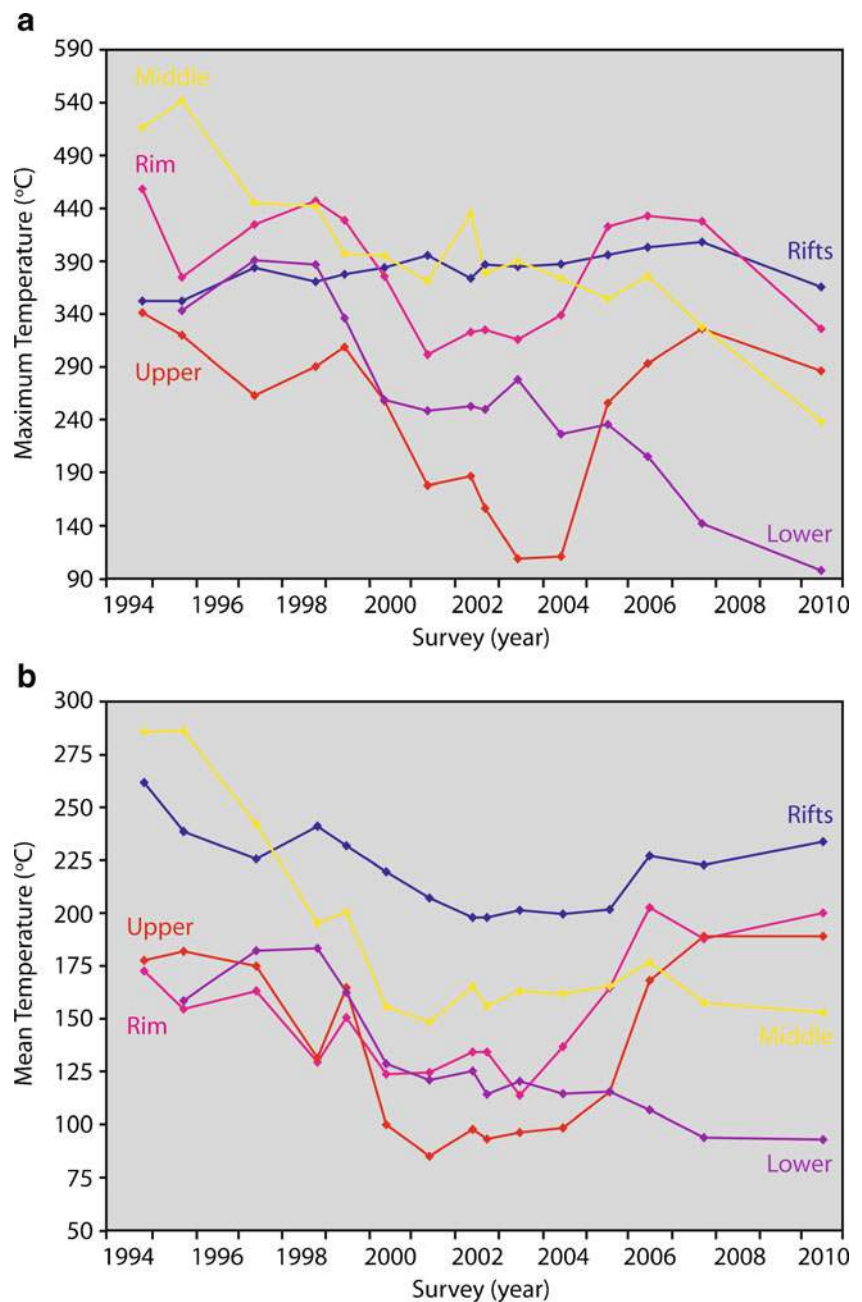
The turnaround did not, however, affect the middle and lower zones, both of which showed a trend of steady decline over the entire 1994 to 2010 period (Fig. 6). In terms of mean temperature, the middle zone appears to have reached

its lowest point by 2001, with the mean temperature remaining fairly stable between this date (at which point it was 150°C) and 2010 (153°C). The lower zone, having declined in mean temperature by 40°C between 1996 and 2001 (Table 5), declined by a further 28°C between 2001 and 2010 (Fig. 6). The decline of the two zones is particularly marked in the maximum temperature plot, with the maximum for the middle zone declining by 150°C between 1994 and 2001, and losing a further 132°C between 2001 and 2010. This crash transformed the middle zone from the first to fourth hottest zone in the field on the basis of both mean and maximum temperature (Fig. 6). Likewise the lower zone, having declined from a maximum of 390°C in 1997 to ~250°C by 2002, declined further to 97°C by 2010 (Fig. 6), at which point the zone was effectively dead showing just a few scattered, boiling point fumaroles. By 2010 the hot ravine on the northwestern edge of the lower zone, as reported in Harris and Maciejewski (2000) and Harris et al. (2009), and located in Fig. 4f, had completely shut down.

#### Spikes

Within these general trends, three single-data-point spikes are apparent, all of which are more evident in the mean temperatures than the maximum temperatures (Fig. 6). The first spike occurred in 1999 and is only apparent in the mean temperature data for the rim, upper and middle zones; the lower zone and rim rifts showed no response. The mean temperature response was most significant at the upper and rim zones which gained 30 and 20°C, respectively, between the 1998 and 1999 surveys, but less so at the middle zone which gained just 5°C. Thereafter, the general declining trend apparent between 1994 and 2001 re-established. The second spike occurred in 2002 and was somewhat weaker, being between 4°C (lower zone), 16°C (middle zone), 13°C

**Fig. 6** Plot of **a** maximum and **b** mean temperature obtained for each zone between 1994 and 2010 (see Tables 2 and 3 for complete data set)



(upper zone) and 9°C (rim zone). However, it did affect all zones apart from the rim rifts. The third spike was apparent in 2006 in the mean temperature data for the middle, rim and rim rift zones (Fig. 6).

#### Histogram analysis

The trends in the mean and maximum temperature data are borne out by an analysis of the frequency distributions generated for the entire field during the period 1994 to 2010 (Fig. 7). Between 1994 and 2000, the distributions lose their high-temperature tails. Instead the distributions develop a more peaked and tightly clustered form, with a

strong low-temperature mode developing in the 80 to 130°C bin by 2000 (Fig. 7). The cooling trend stabilises after 2000, with all distributions during 2000 to 2003 showing a dominant low-temperature mode with a skew towards higher temperatures resulting from the influence of the remaining higher-temperature (>200°C) fumaroles. The warming trend is first evident in 2004 and 2005 and is reflected by the development of an increasingly strong secondary mode in the 180 to 230°C bin, which develops at the expense of the lower-temperature primary mode at 80 to 130°C (Fig. 7). By 2006, heating had developed to such an extent that the primary mode had shifted to the 180 to 230°C bin, with the 80 to 130°C bin now representing a secondary mode

**Table 2** Vent temperature statistics for Vulcano Fossa fumarole field surveys by zone (rim rifts, rim and upper zones) 1994–2010

Year	1994	1995	1997	1998	1999	2000	2001	2002a	2002b	2003	2004	2005	2006	2007	2010
Zone	Rim rifts														
No. of samples	64	33	48	77	80	64	101	119	75	90	67	119	74	75	83.0
Max $T$ (°C)	352	352	383	370	377	383	395	373	386	384	386	395	402	408	364.8
Mean $T$ (°C)	262	239	226	242	232	220	208	198	202	200	215	202	228	223	234.4
Standard deviation	55	79	84	80	67	57	57	63	62	59	66	54	51	47	44.7
Median $T$ (°C)	277	278	244	262	233	216	201	202	200	197	219	203	227	214	233.5
Kurtosis	-0.9	-0.4	-0.9	-0.7	-0.5	0.2	0.9	-0.2	1.2	0.4	0.1	0.7	1.2	2.1	1.5
Skewness	-0.5	-0.7	-0.2	-0.5	-0.2	0.7	0.7	0.2	0.6	0.4	-0.2	0.3	0.3	0.8	0.0
Zone	Rim														
No. of samples	150	96	123	292	167	176	142	188	95	124	116	220	160	175	139
Max $T$ (°C)	457	374	424	446	428	375	301	322	324	315	338	422	432	427	325
Mean $T$ (°C)	173	155	163	130	151	124	125	134	114	137	152	165	203	188	201
Standard deviation	63	73	57	47	50	37	38	39	36	41	45	57	64	52	51
Median $T$ (°C)	163	136	165	115	144	115	114	134	101	138	149	169	199	193	204
Kurtosis	3.9	0.9	5.4	7.9	6.2	12.0	3.7	2.2	11.5	2.4	3.5	2.3	1.9	2.0	-0.2
Skewness	1.6	1.2	1.5	2.1	1.7	2.3	1.5	1.1	3.1	1.1	1.2	1.0	0.9	0.4	-0.4
Zone	Upper														
No. of samples	154	223	63	222	136	63	53	89	54	62	41	67	84	111	71
Max $T$ (°C)	340	319	262	289	308	257	177	185	156	108	110	255	293	325	285
Mean $T$ (°C)	178	182	175	131	165	100	85	98	93	96	98	115	168	196	189
Standard deviation	48	62	49	44	40	26	16	16	14	6	7	43	49	48	48
Median $T$ (°C)	176	189	186	117	165	97	84	94	92	98	99	99	173	201	199
Kurtosis	0.5	-1.1	-1.0	1.1	0.6	20.8	20.9	21.2	8.1	1.1	3.7	2.6	-0.6	0.7	-0.2
Skewness	0.5	0.0	-0.3	1.2	0.4	4.1	3.6	4.3	2.3	-0.9	-1.6	1.9	0.2	-0.2	-0.7

(Fig. 7). Breaking the data set down by zone adds spatial detail to these temporal trends (Fig. 8). The rim rifts

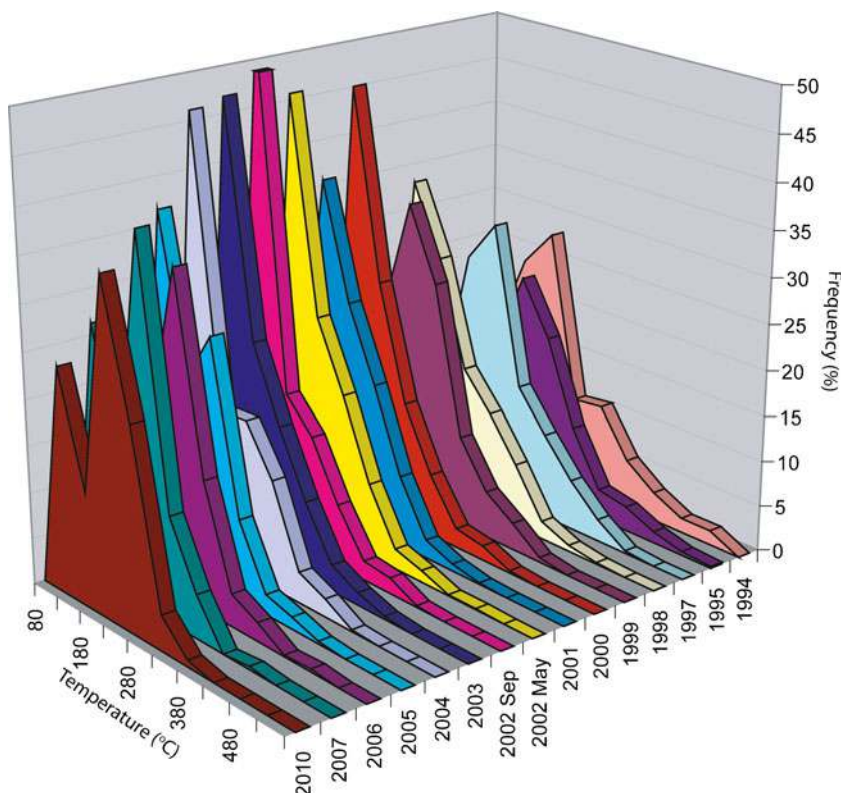
(Fig. 8a) and rim (Fig. 8b) show relatively stable distributions, with features characteristic of a mixed (low- and high-

**Table 3** Vent temperature statistics for Vulcano Fossa fumarole field surveys by zone (middle and lower zones) 1994–2010

Year	1994	1995	1997	1998	1999	2000	2001	2002a	2002b	2003	2004	2005	2006	2007	2010
Zone	Middle														
No. of samples	136	103	334	470	262	336	248	307	177	209	210	191	220	172	84
Max $T$ (°C)	516	541	444	441	396	394	370	434	378	389	373	354	375	327	238
Mean $T$ (°C)	287	287	243	196	201	156	149	165	156	163	162	166	177	158	153
Standard deviation	106	97	74	75	70	66	64	72	75	75	81	66	60	61	52
Median $T$ (°C)	281	278	226	187	185	148	141	163	130	154	108	171	180	161	170
Kurtosis	-0.8	-0.4	-0.7	-0.4	0.0	1.0	-0.3	0.5	0.3	-0.2	-1.0	-0.4	0.1	-0.6	-1.5
Skewness	0.3	0.4	0.5	0.4	0.6	1.0	0.6	0.9	1.0	0.8	0.6	0.5	0.4	0.5	0.0
Zone	Lower														
No. of samples	nd	68	180	152	137	120	98	152	119	97	70	82	53	53	32
Max $T$ (°C)	nd	342	390	386	335	258	248	252	249	277	225	235	204	141	97
Mean $T$ (°C)	nd	159	182	184	163	129	121	125	114	120	114	115	107	94	93
Standard deviation	nd	70	49	64	55	52	49	46	39	46	37	33	25	11	3
Median $T$ (°C)	nd	145	180	171	161	106	106	97	95	95	97	98	97	94	94
Kurtosis	nd	-0.6	2.2	0.1	0.1	0.1	0.1	0.0	1.7	1.3	0.9	2.7	4.2	11.2	2.0
Skewness	nd	0.7	0.6	0.7	0.6	1.1	1.0	1.1	1.5	1.5	1.5	1.7	2.1	2.6	-1.4

Nd no data

**Fig. 7** Frequency distribution of vent temperatures obtained for the entire fumarole field for each survey between 1994 and 2010



temperature) fumarole population. The rim rift distributions, however, show a weaker low-temperature peak (low-to-negative kurtosis) and a stronger high-temperature skew, indicating a more dominant high-temperature population when compared with the rim zone. Both, however, show evidence of cooling during 1994–2000 with stronger low-temperature modes and weaker high-temperature tails after 2000 suggesting an increasing contribution from a low-temperature population. The modal population for the rim rifts shifted from the 280 to 330°C bin during 1994–1998 to the 230 to 280°C bin by 1999 and to the 180 to 230°C bin by 2000; this remained the modal bin until 2010, when heating caused the mode to shift back to the 230 to 280°C bin. Heating had been heralded by the development of a higher-temperature shoulder on the 2007 distribution (Fig. 8a). Heating of the rim after 2002 is apparent from a progressive high-temperature movement of the mode from the 80 to 130°C bin in 2002 to the 130 to 180°C bin during 2003 and 2004. Further heating is apparent from the development of a bi-modal distribution in 2005 and the eventual establishment of a primary mode in the 180 to 230°C bin during all surveys between 2006 and 2010 (Fig. 8b).

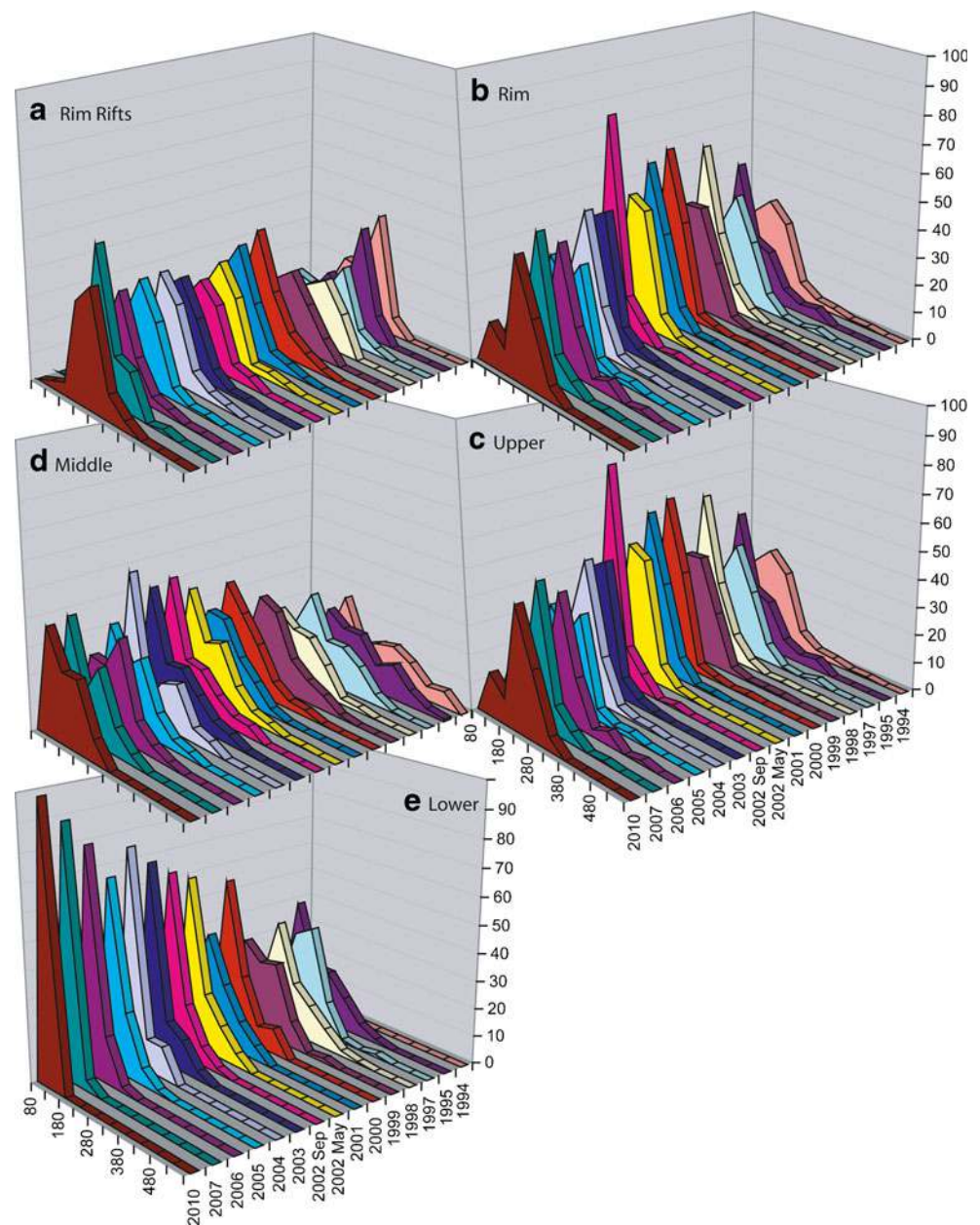
The cooling and heating trends are most marked in the distributions for the upper zone (Fig. 8c), where a dominant, and very stable, low-temperature (80 to 130°C) mode establishes from 2000 onwards. Prior to 2000, the upper zone distribution showed characteristics of a mixed zone of high- and low-temperature fumaroles, but thereafter of a cool

zone, with a distribution tightly clustered around a low-temperature mode and a strongly positive kurtosis. However, heating caused the zone to regain its high-temperature fumarole population in 2006, with the mode shifting to the 180 to 230°C bin at that point (Fig. 8c). The middle zone distribution (Fig. 8d) has shown characteristics of a high-temperature zone throughout the 1994–2010 period, but cooling throughout the period is evident from a weakening of the high-temperature tail, a tightening of the distribution range (evident from the decreased standard deviation, Table 3) and a shift in the modal bin from 180 to 230°C in 1994–1997 to 80 to 130°C by 2007–2010. The lower zone distributions have features characteristic of a mixed (low- and high-temperature) fumarole population until 2000 (Fig. 8e). Again, cooling during the 1994–2000 period is evident from a decay of the high-temperature tail and a strengthening of a low-temperature mode, as reflected by an increase in the kurtosis (Table 4). Since 2000, lower zone distributions have shown evidence of further cooling, with the distribution becoming increasingly tight so that a strong modal population developed in the 80 to 130°C bin (Fig. 8e). This bin, by 2010, contained 100 % of the fumaroles in this zone.

#### Relationship with seismic data

During the period of declining vent temperatures (1994–2000), we note a generally low level of seismic activity in terms of number of events per day, the average being around

**Fig. 8** Frequency distribution of vent temperatures obtained each survey between 1994 and 2010 by zone: **a** rim rifts, **b** rim, **c** upper, **d** middle and **e** lower. Plots are arranged according to the actual spatial position of each zone (i.e. rim is above upper, rim rifts are above middle and middle is above lower)



one event per day (37/month), for a total of 2,686 events, over this 6-year period (Fig. 9a). There is then a gap in the

seismic record until June 2003. Thereafter, we witness a much higher level of seismic activity during the period of

**Table 4** Statistical characteristics of vent temperature data sets collected for low- and high-temperature fumarole zones at Vulcano (from Harris et al. 2009)

Parameter	Low-temperature vent region	High-temperature vent region
Maximum temperature	Low	High
Mean temperature	Low	High
Standard deviation	Low	High
Kurtosis	Positive	Negative
Skewness	Low	High
Characteristic distribution	Tightly clustered distribution, with prominent low-temperature mode	Flatter distribution with wide range of values, heavily skewed towards higher temperatures

**Table 5** Maximum and mean vent temperature difference, by zone, between 1994 and 2001 (except for lower zone where 1996–2001 difference is given)

Zone	Maximum temperature (°C)	Mean temperature (°C)
Rim rifts	+45 (350 to 395)	-50 (260 to 210)
Rim zone	-160 (460 to 300)	-50 (170 to 120)
Upper zone	-160 (340 to 180)	-95 (180 to 85)
Middle zone	-150 (520 to 370)	-140 (290 to 150)
Lower zone	-140 (390 to 250)	-40 (160 to 120)

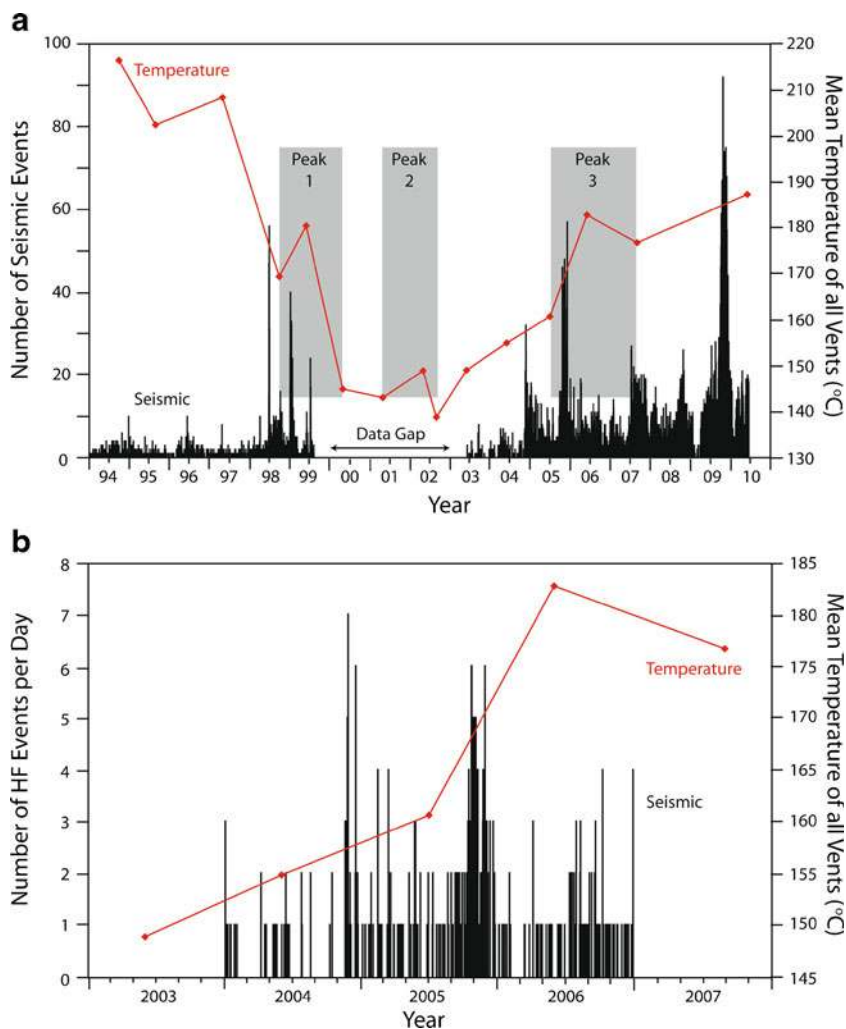
increasing vent temperatures (2003–2010). During the 6-year period spanning 2004–2010, a total of 14,074 events were recorded at an average rate of six events per day (195/month).

Over the 1994–2010 period, the level of seismic activity was not constant, and we observe heightened activity during 1998 and 1999, as well as a series of fluctuations between 2004 and 2010 (Fig. 9a). Two of our three thermal spikes follow such flurries in seismic activity, the June 1999

thermal spike following a January 1999 peak in seismic activity and the June 2006 spike following enhanced seismic activity during November–December 2005. The third thermal spike falls in the data gap of the seismic record.

The plot of Fig. 9a is for all seismic events: long period hybrid (HB), mixed (MB), high-frequency (HF) and monochromatic (MC) events (see Alparone et al. 2010 for definition and Cannata et al. 2012 for their monthly distribution). For the period 2004 to 2007, we are able to distinguish the HF events and see that the thermal spike of June 2006 follows a period of heightened HF activity (Fig. 9b). During September–December 2005, a total of 167 HF events occurred (at an average rate of 42 events per month), compared with a total of 115 HF events over the previous (September 2004–August 2005) 12-month period (average=10 events per month). At the same time, the total number of all seismic events increased from 98 events per month (September 2004–August 2005) to 418 events per month (September–December 2005). Vent temperature changes thus appear related to variations in seismic, especially HF, activity.

**Fig. 9 a** All seismic events (number of events per day) recorded by the Vulcano seismometer network during 1994–2010, with the mean temperature from each of the thermal surveys over-plotted. Each of the short-term peaks in the thermal survey data is located with a *grey box*. **b** Zoom of the 2003–2007 period, i.e. peak three of **a** showing number of high-frequency (HF) events per day, with the mean temperature from each of the thermal surveys over-plotted



## Relationship with deformation data

The distances along lines extending N, W, SW and SE from the Fossa crater for the period 1987 to 2009 are given in Fig. 10. On the W, SW and SE lines, we see extension between 1987 and 1997. Extension is especially marked for points linking each base station and the furthest point on the line, i.e. points on the Fossa cone itself. For these lines, extension by between 4 and 10 cm is apparent which follows a linear temporal trend. No trend is observed on the northern line. Extension of the line means contraction of the source (so that it moves away from the reference point). Because this movement affects points on the Fossa cone only and does not affect the northern line, we can infer that the Fossa's western and southern sectors experienced contraction during 1987–1997. Thereafter, we see no movement

on any line, indicating no deformation between 1997 and 2009.

The extension phase of 1990–1996 has already been considered by Gambino and Guglielmino (2008) who, by assuming a deflation–inflation source centred on the Fossa cone, were able to explain line extension in terms of deflation and contraction of the cone. Contraction was consistent with a  $\sim 0.5 \times 10^5\text{-m}^3$  decrease in volume for a source located at a depth of 254 m (Gambino and Guglielmino 2008). Because this contraction occurred during the 1979–1995 period of fumarole field heating and expansion, Gambino and Guglielmino (2008) proposed that heating caused increased water evaporation, reducing the bulk volume of the shallow hydrothermal system, to result in deflation and contraction. Hence, high temperatures and heating should be associated with contraction.

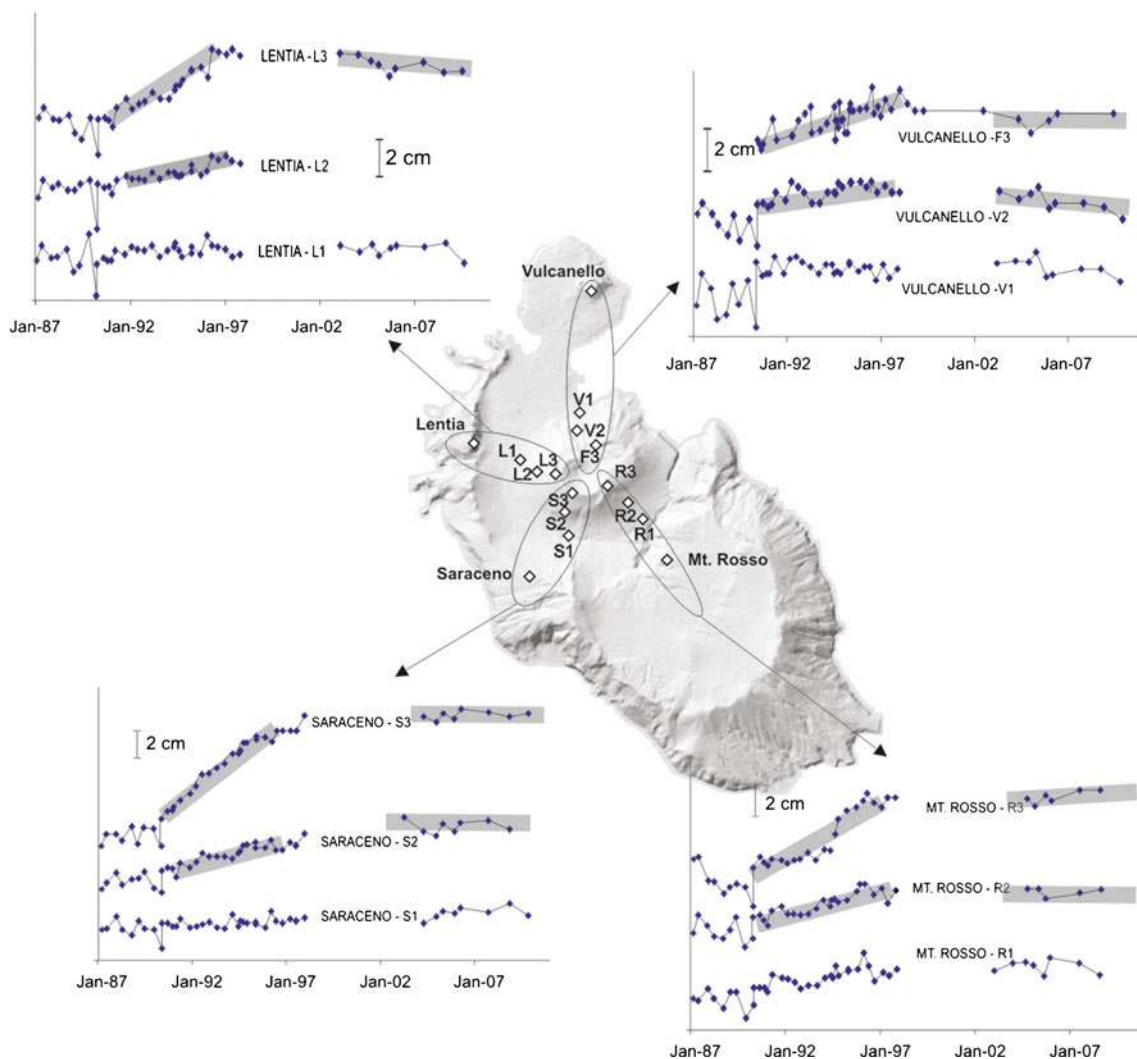


**Fig. 10** Changes in measured distance along lines connecting the benchmarks positioned on the Fossa cone and the stable benchmarks as function of time (1987–2009). Distance measurement errors are less

than  $\pm 7$  mm; the two grey zones mark the periods of deflation (line lengthening) and stability (no deformation), respectively

## Fumarole migration and vent temperature variation

During the peak temperature phase of the early 1990s, new high-temperature fumaroles developed in the middle zone (at FA), and later across the lower zone. The historical zone of activity along the rim remained active but, as of 1994, was the coolest zone by mean temperature. The period of vent temperature decline that followed spanned 1994 and 2000 and affected all zones, although the lower zone was late to start its turn around, not beginning to show a decline in mean temperature until 1998. By 2003, upper zone vent temperatures had decreased, and fumaroles had shut down, to such an extent that it was effectively dead. The vent temperature decline was least felt at the rim rifts, so that the rim rifts took over as the hottest zone in the field (by mean temperature) during 1998, a position which this zone maintained through 2010. A new phase of vent temperature increase began at the rim zone, with the turnaround being underway by 2004. The upper zone resurrected during the following year (2005), and the rim rifts followed after another year (2006). The middle and lower zones did not respond and instead continued to show a declining trend, so the lower zone was effectively dead by 2010. Thus, our vent temperature surveys indicate a migration of activity from the middle and lower zones towards the rim during 2004–2010. This reverses the direction of movement that occurred during the heating episode of the early 1990s.

### The role of permeability

Two of the three spikes observed in our vent temperature time series follow (by ~6 months) periods of heightened seismic activity (the third spike falls in a seismic data gap). Heightened seismic periods were characterised by an increase in all types of seismic events, including high-frequency events. At the Fossa, such HF events have been associated with rock fracturing at between 200 and 1,600 m below sea level (Alparone et al. 2010). This leads us to propose that vent temperatures are strongly influenced by fracturing, with vent temperatures increasing as fractures open and shallow system permeability increases. Our assessments are consistent with Cannata et al. (2012), who also consider permeability changes as a possible cause for the 2004–2007 increases in both temperature and seismicity at Vulcano. In particular, we believe that a cyclic sealing–fracturing process, whereby pathways steadily seal until pore pressure exceeds a critical value, may be envisaged for such events. Build up of pore pressure beneath a sealing zone triggers a fracturing episode, a flurry of HF activity and a spike in vent temperatures. Initial gas pressures, fluxes and temperatures are high as the pressurized source is tapped, but wane as the source is depressurised. This allows vent temperature to decline, sealing to recommence and the cycle to resume.

Fractures will seal as temperatures drop. Precipitation of sulphur, for example, becomes much more effective at decreased temperatures, especially as temperatures drop below 100°C (Harris and Maciejewski 2000). Such a process will steadily block pathways used by the ascending fluid flux and its associated heat. If a zone seals sufficiently, it is easier for ascending fluids to utilise a more permeable pathway. If a zone becomes sufficiently sealed and more permeable zones are available, the low permeability zone will be abandoned in favour of the high permeability zone. The effect is not immediate. We see gradual vent cooling and abandonment of sealing zones and equally gradual enhancement of vent temperatures at permeable zones. Our temperature data show that, at Vulcano, expansion and contraction of the exhaling area, coupled with sealing–fracturing process operating in the shallow system (within 1,600 m of the surface—the location of the HF events) steadily pushed the surface expression of the ascending fluid (and heat) flux towards the crater floor between 1998 and 1994 and then back towards the crater rim during 2003–2010.

### Causes of shallow system heating and cooling

We witness a phase of apparent heating, as expressed by increased vent temperatures, beginning around 2004. During this phase, we also see increased seismic activity with no deformation. This is in contrast with the heating phase of 1986–1993 which was associated with deflation due to evaporation of water in the high-temperature system (Gambino and Guglielmino 2008). We thus propose that the increase in vent temperature between 2004 and 2010 was not driven by an enhanced flux of fluids and heat from the deep source because this would have been associated with drying out of the system and deflation. Instead, following the reasoning of the previous section, we suggest that increased temperatures were related to changes in the permeability of the shallow system, with increased permeability allowing more efficient fluid and heat ascent. Within this model, fracturing generates increased HF seismic activity, opens up the permeability and increases gas and heat flux and thus vent temperatures. With an increasingly open system, there is no pressurization or inflation. Neither, though, is there heating, so there is also no deflation.

Vent temperature increases after 2004 affected mostly the upper and rim zones, with the middle zone undergoing reduced activity and the lower zone being abandoned altogether. A change in the spatial distribution of vent temperatures thus occurred in a direction away from the newer zones, which had opened up during the heating phase of 1979–1995 and towards traditionally active and highly fractured zones at the rim. These are also the zone of preferential fumarolic emission predicted by the stress field model of Schöpa et al. (2011). With cooling, the dying lower and

middle zones became rapidly sealed and abandoned; the upper and rim zones, in contrast, opened up as the ascending flux was diverted towards them. Rejuvenation of the upper and rim zones by fracturing is consistent with the increased HF events recorded over the same period and, as discussed above, likely resulted from increased pore pressure across the upper and rim zones due to diversion of the flux from the sealing lower and middle zones.

That we see increased vent temperatures between 2004 and 2010 across the upper and rim zones is thus not necessarily associated with heating of the system but instead by decreased permeability across certain zones and increased permeability to others. This allows more efficient heat transport across zones where stress conditions are more favourable to fluid ascent (Schöpa et al. 2011). Alparone et al. (2010) also observe the gradual evolution in seismic waveforms during 2004–2006. This evolution was argued to be indicative of heating and drying of the hydrothermal system. As already discussed, we see an increase in HF events followed by a phase of vent temperature increase, consistent with opening of fractures and increased permeability across reactivated zones. However, we also see increased numbers of HB, MB and MC events after 2004. Such events are not associated directly with fracturing processes but instead can be explained by crack resonance (Alparone et al. 2010). A persistent increase in their incidence between 2004 and 2010 thus seems to suggest increased flow of hot, gas-rich fluids towards the surface, which facilitates the fracturing process through increased pore pressure (Alparone et al. 2010). Again, because this process was not associated with deformation, we argue that there was no new or enhanced input from the deep source, just a spatial re-organisation of the system due to changing permeability conditions, with higher permeability allowing increased fluid flow towards the northern (rim) sector of the fumarole field.

## Model

Our combined thermal, seismic and deformation data sets thereby support a permeability-driven model in which variations in vent temperature and location across Vulcano's Fossa crater during 1994–2010 were forced from the top-down. In short, changing permeability conditions modified the ability of fluids and their associated heat to ascend and resulted in zonal shut down, rejuvenation and re-organisation of the spatial distribution of vent temperatures. Our model is given in Fig. 11. It shows the location of the heated, deflating source of Gambino and Guglielmino (2008), where the lack of deformation during 2004–2010 leads us to assume that this source was inactive by this period. The model allows us to define two types of heating phases at Vulcano,

“real” and “apparent”, which developed over three thermally defined phases between 1986 and 2010:

### 1. Phase 1: real heating phase—1986–1993

During periods of “real” heating, the fumarole field experiences vent temperature increases and movement. With increased flux of fluids and heat from the deep source, the system expands and low permeability zones at the margin of the chimney of ascending fluids are occupied. In the case of the 1986–1993 crisis, movement was progressively towards the crater floor, with first the middle zone, and then the lower zone, opening up. Heating caused increased vent temperatures, field expansion and drying out of the system underneath the newly established hot zone to cause deflation.

### 2. Phase 2: cooling phase—1994–2003

With cooling, the field begins to shrink. The marginal zones occupied during the heating phase are progressively abandoned, as was the heated source of Gambino and Guglielmino (2008). Movement during the cooling phase is thus in the opposite direction to that experienced during the heating phase, i.e. towards the crater rim, with the last zone to be occupied (the lower zone) being the first to be abandoned. As cooling progresses, vent temperatures decline and the location of dominant emission becomes re-established at the crater rim, as the marginal (lower) zones die and seal.

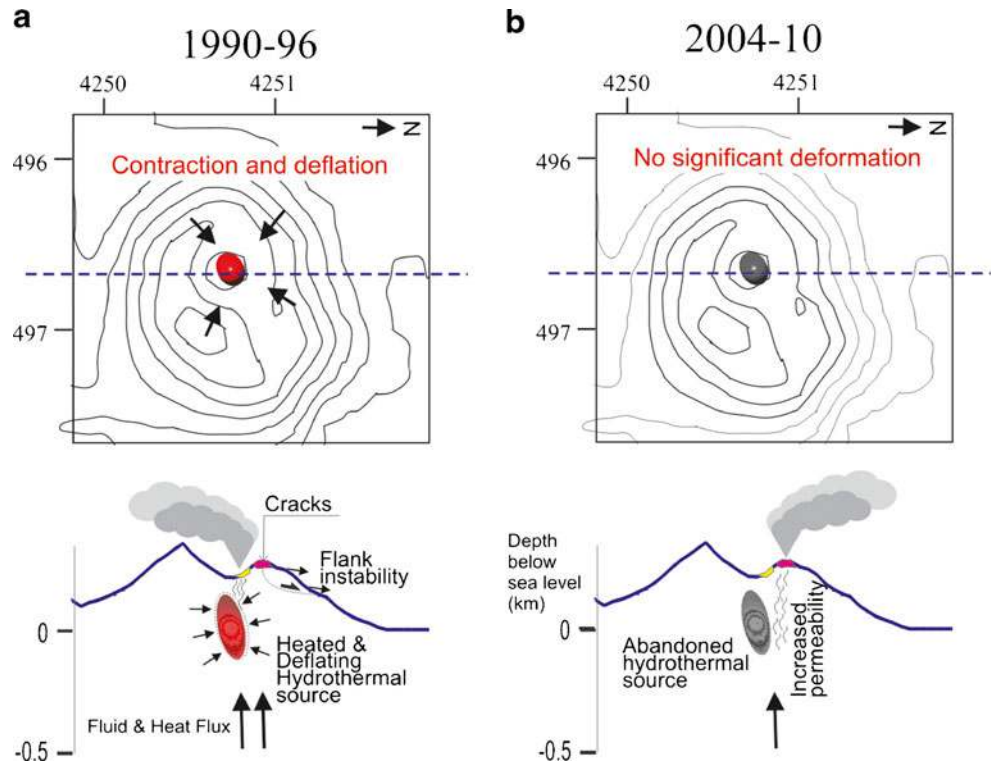
### 3. Phase 3: apparent heating phase—2004–2010

Enhanced fluid and heat flow towards the core (rim) zone results in increased pore pressure fracturing and increased incidence of HF seismic events, as well as signals associated with enhanced fluid flow in the rejuvenated zones. Vent temperatures respond by increasing across the rejuvenated zones, but the absence of pervasive heating is reflected by an absence of deflation, implying that the system is not drying out. However, inflation is also not observed because fracturing makes the system permeable and open. Hence, the heating phase is in fact “apparent” because it is simply a re-organisation of vent temperatures forced by the changed permeability conditions.

## Importance, and potential, of heat flux measurements

This analysis highlights the importance of measuring heat flux, and we need to define the difference between tracking fumarole temperature (recorded for a single vent) and heat flux (obtained from a survey of all vents across the entire fumarole field). If a heating event involves higher temperatures recorded at the maximum temperature vent, but the size of the fumarole field decreases (i.e. we have fewer vents), the “apparent heating” vent may not be associated with a higher overall heat flux. On the other hand, if a

**Fig. 11** Plan and north–south cross section through the Fossa cone and a generalized model of the fumarolic system during **a** 1990–1996 and **b** 2004–2010. Coordinates are UTM projection (kilometres), zone 33 N; contours increase in increments of 100 m. Instability of the Fossa’s NE flank during the 1990–1996 period is inferred from Bonaccorso et al. (2010). The ephemeral hydrothermal source whose heating and cooling drives the deformation pattern and activation, and deactivation, of the lower fumarole zones in the crater is placed following Gambino and Guglielmino (2008)



cooling event is recorded by lower temperatures at the monitored vent, but the size of the field increases (i.e. we have greater number of vents), the “apparent cooling” may be associated with an increased overall heat flux. Thus, fumarole-field-wide vent temperature measurements are needed to check the heat flux during times of apparent heating or cooling (Harris and Maciejewski 2000). That is, if the vent temperature at a single target fumarole is increasing, is the total heat flux also increasing? If the answer is “no,” then we have an apparent heating event as is the case here.

Monitoring of single high-temperature fumaroles can thus indicate apparent heating or cooling, but such trends need to be checked against, or confirmed by, field-wide heat flux measurements. Here, we use annual infrared thermometer-based field surveys to identify general trends in fumarole field state (i.e. cooling versus heating). Another way to obtain fumarole-field-wide heat fluxes is through satellite-based thermal measurements (e.g. Gaonac’h et al. 1994; Harris and Stevenson 1997). However, the hot spots associated with the small, sub-pixel, vents scattered across a fumarole field can make thermal infrared measurements with even the best spatial resolution satellite data, i.e. the 60-to-120-m-pixel data obtained by satellite sensors such as TM, ETM+ or ASTER, challenging (Harris and Stevenson 1997). Thermal maps and heat flux estimates made using thermal camera data are a potential option (e.g. Matsushima et al. 2003; Harris et al. 2009; Schöpa et al. 2011). Such methodologies can be applied

to data acquired by permanently recording cameras, as have been installed at Vulcano (Lodato et al. 2008). Heat flux extractions from thermal image data collected every few minutes would allow heat flux tracking at high temporal resolutions, resolutions that match those currently made at single, permanently monitored fumaroles. Such measurements should be coupled with measurements of heat carried by the gas phase and/or soil heating, where our estimates indicate that 27 % of the heat flux at Vulcano is accounted for by heat losses at open vents, as can be measured using infrared sensors, the remainder being accounted for by diffuse heat losses (Harris et al. 2009). The latter heat flux can be obtained through appropriate measurement of gas (mostly water) flux and/or placement of thermal sensors buried in the soil (e.g. Chiodini et al. 2005; Aubert et al. 2008).

## Conclusions

During the 16 years spanning 1994 and 2010, we recorded an 8-year period of vent temperature decline followed by an 8-year period of increase. These fumarole-field-wide temperature trends are supported by the same trends apparent in higher-frequency temperature records for single fumaroles within the field, as presented by Diliberto (2011) for the period 1998–2010. This oscillation has to be set in the context of decadal scale variations in the thermal state of

Vulcano's system, where oscillations of a similar time scale have previously been observed in the 1920s and the 1980s/1990s. These thermal oscillations were associated with heating phases during which activity across both the magmatic and hydrothermal systems increased (Barberi et al. 1991). This increase was generally associated with enhanced fluxes of magmatic fluids from the deep source (Carapezza et al. 1981; Bolognesi and D'Amore 1983; Cioni and D'Amore 1984; Mazar et al. 1988; Chiodini et al. 1993, 1995).

However, we find that the most recent phase of vent temperature increase (2002–2010) was driven by changes in the shallow system permeability conditions. This is consistent with the model of Todesco et al. (2010) which shows how increases in system permeability can promote increased heat, gas and fluid flow through the system, without requiring a change in the flux of magmatic fluids from the deep source. It is also consistent with the relation found between seismic activity, ground deformation, soil temperature and fumarole temperature data recorded at Vulcano by Cannata et al. (2012) during the period 2004–2007. During this time, four 3-to-5-month-long temperature increases were recorded for single fumaroles and especially at a single soil temperature station (where soil temperature was measured at a depth of 10 cm). These thermal anomalies were coincident with increased numbers of volcano seismic events associated with resonance and shear failure. Cannata et al. (2012) suggested that this relation could be explained by “increases in the release of gas from a deep and stable magma body, without magma intrusion,” with changes in rock permeability being proposed as one mechanism by which the heat flux could be enhanced without new intrusion.

Permeability, and likely also the evolution of sealed zones in cooling sectors of the fumarole field, strongly influences the final destination of ascending fluid and heat fluxes. The current configuration of Vulcano's Fossa fumarole field means that ascending fluids, and their associated heat, encounter a sealed zone towards the lower portion of the crater and is diverted to, and thus preferentially released from, traditionally active zones towards the rim. These zones undergo a degree of rejuvenation by fracturing, so that increased vent temperature is a function of increased pore pressure which induces fracturing to clear out pathways and increase system permeability. The preferred pathway of the rim rift and rim zones suggest that these areas are more highly fractured and permeable, a situation which may result from a structural control forced by the location of older crater boundaries, as well as stress field conditions (Schöpa et al. 2011).

Our study links fumarole-field-wide thermal surveys with seismic and deformation data to generate a robust model for the temporal and spatial dynamics of Vulcano's fumarole field that might be applied also to volcanic hydrothermal systems with similar geophysical characteristics. Each data

set points to a similar conclusion providing different, but mutually supportive, lines of evidence:

- (a) The seismic data indicate increased fracturing.
- (b) Deformation data indicate contraction due to heating and evaporation, or no deformation during highly permeable conditions.
- (c) Mapping temperatures across the entire fumarole field reveals migration of active vents which can be related to the field's history of sealing and fracturing.

We find that the field pushes its source of preferential emission into new zones as real thermal crises evolve. The same zones shut down and mature zones rejuvenate as the heating phase wanes. The diversion of fluid fluxes increases pore pressure, enhances fracturing and increases permeability in the rejuvenated zones to create vent temperature increases without a change in the input deep magmatic source. This process is capable of generating “apparent heating” phases that can only be interpreted using a fully integrated geophysical data set.

**Acknowledgments** We acknowledge the work and support of the Gruppo Analisi Dati Sismici and the staff of the periodic GPS surveys group of INGV, Sez. Catania (Osservatorio Etno). AH is indebted to the hospitality of La Giara.

The authors acknowledge the helpful suggestions and support of the two reviewers: Laszlo Kestay and anonymous. AH was supported by la Région Auvergne. This is Laboratory of Excellence ClerVolc contribution no. 20.

## References

- Alparone S, Cannata A, Gambino S, Gresta S, Milluzzo V, Montalto P (2010) Time–space variation of volcano-seismic events at La Fossa (Vulcano, Aeolian Islands, Italy): new insights into seismic sources in a hydrothermal system. *Bull Volcanol* 72:803–816
- Aubert M, Diliberto S, Finizola A, Chébli Y (2008) Double origin of hydrothermal convective flux variations in the Fossa of Vulcano (Italy). *Bull Volcanol* 70:743–751
- Barberi F, Neri G, Valenza M, Villari L (1991) 1987–1990 unrest at Vulcano. *Acta Vulcanol* 1:95–106
- Bolognesi L, D'Amore F (1983) Isotopic variation of the hydrothermal system on Vulcano Island, Italy. *Geochimica et Cosmochimica Acta* 57:2069–2082
- Bonaccorso A, Bonforte A, Gambino S (2010) Thermal expansion–contraction and slope instability of a fumarole field inferred from geodetic measurements at Vulcano. *Bull Volcanol*. doi:10.1007/s00445-010-0366-7
- Bonforte A, Guglielmino F (2008) Transpressive strain on the Lipari–Vulcano volcanic complex and dynamics of the “La Fossa” cone (Aeolian Islands, Sicily) revealed by GPS surveys on a dense network. *Tectonophysics* 457:64–70. doi:10.1016/j.tecto.2008.05.016
- Bukumirovic T, Italiano F, Nuccio PM, Pecoraino G, Principio E (1996) Evolution of the fumarolic activity at La Fossa crater of Vulcano. *Acta Vulcanol* 8:210–212
- Bukumirovic T, Italiano F, Nuccio PM (1997) The evolution of a dynamic geological system: the support of a GIS for geochemical measurements at the fumarole field of Vulcano, Italy. *J Volcanol Geotherm Res* 79:253–263

- Capasso G, Inguaggiato S, Nuccio PM, Pecoraino G, Sortino F (1994) Chemical variations in the fumarolic gases of La Fossa di Vulcano crater. *Acta Vulcanol* 4:41–43
- Cannata A, Diliberto S, Alparone S, Gambino S, Gresta S, Liotta M, Madonia P, Milluzzo V, Aliotta M, Montalto P (2012) Multiparametric approach in investigating volcano-hydrothermal systems: the case study of Vulcano (Aeolian Islands, Italy). *Pure App Geophy* 169:167–182. doi:10.1007/s00024-011-0297-z
- Carapezza M, Nuccio PM, Valenza M (1981) Genesis and evolution of the fumaroles of Vulcano (Aeolian Island Italy). *Bull Vulcanol* 44:547–563
- Chiodini G, Cioni R, Guidi M, Marini L, Raco B, Taddeucci G (1992a) Gas geobarometry in boiling hydrothermal systems: a possible tool to evaluate the hazard of hydrothermal explosions. *Acta Vulcanol* 2:99–107
- Chiodini G, Cioni R, Falsaperla S, Montalto A, Guidi M, Marini L (1992b) Geochemical and seismological investigations at Vulcano (Aeolian Islands) during 1978–1989. *J Geophys Res* 97(B7):11025–11032
- Chiodini G, Cioni R, Marini L (1993) Reactions governing the chemistry of crater fumaroles from Vulcano Island Italy, and implications for volcanic surveillance. *Appl Geoch* 8:357–371
- Chiodini G, Cioni R, Marini L, Panichi C (1995) Origin of the fumarolic fluids of Vulcano Island, Italy, and implication for volcanic surveillance. *Bull Vulcanol* 57:99–110
- Chiodini G, Granieri D, Avino R, Caliro S, Costa A (2005) Carbon dioxide diffuse degassing and estimation of heat release from volcanic and hydrothermal systems. *J Geophys Res* 110: B08204. doi:10.1029/2004JB003542
- Cioni R, D'Amore F (1984) A genetic model for the crater fumaroles of Vulcano Island (Sicily, Italy). *Geothermics* 13:375–384
- Diliberto IS (2011) Long-term variations of fumaroles temperatures on Vulcano Island (Italy). *Ann Geophys* 54:175–185
- Falsaperla S, Frazzetta G, Neri G, Nunnari G, Velardita R, Villari L (1989) Vulcano monitoring in the Aeolian Islands (Southern Tyrrhenian Sea): the Lipari–Vulcano eruptive complex. In: Latter JH (ed) *Volcanic hazards: assessment and monitoring IAVCEI Proceedings in Volcanology 1*. Springer, New York, pp 337–356
- Gambino S, Guglielmino F (2008) Ground deformation induced by geothermal processes: a model for La Fossa Crater (Vulcano Island, Italy). *J Geophys Res* 113:B07402. doi:10.1029/2007JB005016
- Gaonac'h H, Vandemeulebrouck J, Stix J, Halbachs M (1994) Thermal infrared satellite measurements of volcanic activity at Stromboli and Vulcano. *J Geophys Res* 99(B5):9477–9485
- Granieri D, Avino R, Carapezza ML, Chiodini G, Ranaldi M, Ricci T, Tarchini L (2006) Correlated increase in CO<sub>2</sub> fumarolic content and diffuse emission from La Fossa crater (Vulcano, Italy). Evidence of volcanic unrest or increasing gas release from a stationary deep magma body? *Geophys Res Lett* 33:L13316. doi:10.1029/2006GL026460
- Giustolisi V, de Oliveira HA (2005) *Bibliografia generale delle Isole Eolie: Vulcano*. Centro di Documentazione e Ricerca per La Sicilia Antica “P. Orsi”—Onlus (Palermo), p 216
- Hardee HC (1982) Permeable convection above magma bodies. *Tectonophysics* 84:179–195
- Harris AJL, Maciejewski AJH (2000) Thermal survey's of the Vulcano Fossa fumarole field 1994–1999: evidence for fumarole migration and sealing. *J Volcanol Geotherm Res* 102(1–2):119–147
- Harris AJL, Stevenson DS (1997) Thermal observations of degassing open conduits and fumaroles at Stromboli and Vulcano using remotely sensed data. *J Volcanol Geotherm Res* 76:175–198
- Harris AJL, Lodato L, Dehn J, Spampinato L (2009) Thermal characterization of the Vulcano fumarole field. *Bull Vulcanol* 71:441–458
- Italiano F, Nuccio PM, Valenza M (1984) Geothermal energy and mass release at Vulcano, Aeolian Island, Italy. *Rend Soc Ital Min Petrol* 39:379–386
- Italiano F, Nuccio P (1992) Volcanic steam output directly measured in fumaroles: the observed variations at Vulcano Island Italy, between 1983 and 1987. *Bull Vulcanol* 54:623–630
- Lodato L, Spampinato L, Harris AJL, Dehn J, James MR, Pecora E, Biale E, Curcuruto A (2008) Use of forward looking infrared thermal cameras at active volcanoes. In: Marzocchi W, Zollo A (eds) *Conception, verification and application of innovative techniques to study active volcanoes*. Istituto Nazionale di Geofisica e Vulcanologia, Italy, pp 427–434
- Martini M, Giannini L, Capaccioni B (1991a) The influence of water on chemical changes of fumarolic gases: different characters and their implications for forecasting volcanic activity. *Acta Vulcanol* 1:13–16
- Matsushima N, Kazahaya K, Saito G, Shinohara H (2003) Mass and heat flux of volcanic gas discharging from the summit crater of Iwodake volcano, Satsuma-Iwojima, Japan, during 1996–1999. *J Volcanol Geotherm Res* 126:285–301
- Martini M, Giannini L, Capaccioni B (1991b) Geochemical and seismic precursors to volcanic activity. *Acta Vulcanol* 1:7–11
- Mazor E, Cioni R, Corazza E, Fratta M, Magro G, Matsuo S, Hirabayashi J, Shinohara H, Martini M, Piccardi G, Cellini-Legittimo P (1988) Evolution of fumarolic gases—boundary conditions set by measured parameters: case study at Vulcano, Italy. *Bull Vulcanol* 50:71–85
- Oppenheimer CMM, Rothery DA (1991) Infrared monitoring of volcanoes by satellite. *J Geol Soc Lon* 148:563–569
- Schöpa A, Pantaleo M, Walter TA (2011) Scale-dependent location of hydrothermal vents: stress field models and infrared field observations of the Fossa Cone, Vulcano Island, Italy. *J Volcanol Geotherm Res* 203:133–145
- Sicardi L (1940) Il recente ciclo dell'attività fumarolica dell'isola di Vulcano. *Bull Vulcanol* 7:85–140
- Stevenson DS (1993) Physical models of fumarolic flow. *J Volcanol Geotherm Res* 57:139–156
- Todesco M, Rinaldi AP, Bonafede M (2010) Modeling of unrest signals in heterogeneous hydrothermal systems. *J Geophys Res* 115:B09213. doi:10.1029/2010JB007474